(55 to 85 days) hatching does not commence until a few days after return to 15°C.

Newly hatched polyps rapidly grow to full size and bud vigorously whether they are maintained at 15° or 24°C. The derived populations are refractory to sex induction for approximately 120 days during which period they continue to bud after transfer from 24° to 15°C. Thus, although 15°C is required for the realization of the sexual state, a prior and relatively long period of asexual activity is also mandatory for the induction of the sexual phase of the life-cycle. The original material was collected in the fall and can be assumed to have spent the preceding summer months in the asexual state.

Time plays a critical role in two phases of the life-cycle. First, exposure of the embryos to 4°C initiates the processes leading to normal and synchronous hatching, but no hatching occurs until after return to 15°C, an indication that embryos produced in the fall will not hatch until the next spring. Second, newly hatched polyps are refractory to sex induction for a long period roughly equivalent to the duration of the summer months. Such a regulatory mechanism is well adapted to produce a regular alternation of reproductive modes, especially in north temperate regions where seasonal variation in environmental temperature is the rule.

JOHN DAVISON

Department of Zoology,
University of Vermont,
Burlington 05401

References and Notes

1. P. Tardent, *Am. Zool.* **14**, 447 (1974); *Rev. Suisse Zool.* **73**, 357 (1966); *Dev. Biol.* **17**, 483 (1968); H. D. Park, C. Mecca, A. Ortmeyer, *Biol. Bull. Woods Hole, Mass.* **126**, 121 (1964); P. Brien, *Am. Sci.* **48**, 461 (1960).
2. H. D. Park, N. E. Sharpless, A. B. Ortmeyer, *J. Exp. Zool.* **160**, 247 (1965).
3. H. Forrest, *Trans. Am. Microsc. Soc.* **82**, 6 (1963); R. W. Pennak, *Freshwater Invertebrates of the United States* (Ronald, New York, 1953).
4. J. Davison, *J. Gen. Physiol.* **53**, 562 (1969); *ibid.* **61**, 767 (1973).

7 June 1976

High Concentration of GABA and High Glutamate Decarboxylase Activity in Rat Pancreatic Islets and Human Insulinoma

Abstract. *The concentration of γ-aminobutyric acid (GABA) and the activity of glutamate decarboxylase (GAD) in rat and human pancreas were measured by sensitive assay methods. The GABA concentration in rat pancreas was 2.51 millimoles per kilogram (dry weight) and GAD activity was 2.58 mmoles per kilogram per hour. The GABA concentration and GAD activity in rat Langerhans' islets were 18.9 mmole kg^{-1} and 66.7 mmole kg^{-1} $hour^{-1}$, whereas those in the exocrine acini were 1.97 mmole kg^{-1} and 4.67 mmole kg^{-1} $hour^{-1}$, respectively. In an insulinoma region of human pancreas the GABA concentration was 25.5 mmole kg^{-1} and the GAD activity was 138.2 mmole kg^{-1} $hour^{-1}$, but in the surrounding nontumor region these values were only 2.81 mmole kg^{-1} and 2.01 mmole kg^{-1} $hour^{-1}$, respectively, similar to the values in normal rat pancreas.*

Since the discovery of γ-aminobutyric acid (GABA) in mammalian brain in 1950 many studies of its function and metabolism have been carried out (*1*). While there is now good evidence that GABA is an inhibitory neurotransmitter in the mammalian brain as well as in the invertebrate central nervous system (CNS) (*2, 3*), there is also evidence that GABA as well as glutamate decarboxylase (GAD) occur in nonneuronal tissues such as kidney, liver, and adrenal gland (*4, 5*), although at much lower concentrations than in nerve tissue. Tallan *et al.* (*6*) and Drummond *et al.* (*7*) also found a very small amount of GABA in pancreas, although their assay method seemed not to be sensitive enough to measure the exact amount of the compound in the tissue. We found previously a high concentration of GABA in Langerhans' islets of rat pancreas (*8*). In the studies reported here, GAD activity and GABA concentration were determined in rat pancreas, rat pancreatic endocrine and exocrine glands, and in insulinoma of human pancreas by means of a sensitive assay method (*9*).

Albino rats weighing 85 to 100 g were anesthetized with pentobarbitone sodium (50 mg kg^{-1}), the abdominal cavity was opened, and the pancreas together with exocrine and endocrine glands was carefully removed. The tissue was immediately immersed in Freon-12 and chilled to its freezing point (−150°C) in liquid nitrogen. The tissue block was cut with a microtome in a cryostat (−20°C), and serial sections (15 to 20 μm) were freeze-dried overnight at −30°C in a vacuum. For the determination of GABA and GAD in whole pancreas (exocrine plus endocrine glands), two or three sections of freeze-dried tissue (100 to 200 μg) were used. For the assay of GABA and GAD separately in the endocrine and exocrine glands, the Langerhans' islets and acini were isolated with a fine dissecting knife under a stereomicroscope. The islets of Langerhans were well differentiated from the exocrine gland. Each isolated islet and exocrine sample was weighed with a fish-pole quartz fiber balance. The weight of a single islet ranged from 40 to 60 ng and that of the exocrine area from 40 to 200 ng.

For the assay of GABA (direct method) in whole, freeze-dried sections of pancreas, each sample was transferred to a 2-ml fluorometer tube, and 20 μl of 0.01*N* HCl was added; the sample was then heated at 60°C for 10 minutes to destroy enzyme activity and endogenous reduced nicotinamide adenine dinucleotide phosphate (NADPH). The freeze-dried sample was easily dissolved by this treatment. After the addition of 80 μl of GABA assay reagent, the samples were incubated at 38°C for 30 minutes. The GABA assay reagent consisted of 0.3*M* tris-HCl buffer (*p*H 8.9), 10 m*M* α-ketoglutarate, 1 m*M* NADP, 0.01 percent mercaptoethanol, and 60 μg of protein per milliliter of bacterial-derived enzymes: γ-aminobutyrate aminotransferase (E.C. 2.6.1.19) and succinate semialdehyde dehydrogenase (E.C. 1.2.1.16). After incubation, the reaction mixture was diluted to 1.0 ml with 0.1*M* tris-HCl buffer (*p*H 8.0) to stop the reaction. The fluorescence of the NADPH was determined by means of a Farrand fluorometer.

For the GAD assay (direct method) the tissue sample was transferred to 30 μl of GAD assay reagent in a fluorometer tube and incubated at 38°C for 60 minutes. The GAD assay reagent consisted of 0.1*M* phosphate buffer (*p*H 6.8), 50 m*M* glutamate, 250 μ*M* pyridoxal phosphate, and 0.2 percent mercaptoethanol. After incubation, the samples were heated at 100°C for 2 minutes to stop the reaction. The mixture was incubated at 38°C for 30 minutes after adding 80 μl of GABA assay reagent. Then 0.8 ml of 0.1*M* tris-HCl buffer was added and the fluorescence of the NADPH produced was determined in the fluorometer. To calculate the GAD activity, endogenous GABA was subtracted from the total GABA value obtained after 60 minutes of incubation with the GAD assay reagent.

For the microassay of GABA and GAD from an isolated single islet and small area of acinus, an oil-well tech-

nique and the enzymatic cycling method for NADPH (*10*) were employed. The principles and the detail of the assay methods have been described (*9*). In this experiment, the enzymatic cycling rate of NADPH was adjusted to 2000 cycles per hour for the GAD assay and 5000 to 7000 cycles per hour for the GABA determination. At least six different standards were run in each assay.

The concentration of GABA and the activity of GAD in rat pancreas (see Table 1, measurement 1) was high compared with other nonneuronal tissues such as liver and kidney (*5, 6*). Recently, the presence of GABA in rat pancreas was confirmed by dansylation (with 1-dimethylaminonaphthaline-5-sulfonyl chloride) and mass spectroscopic methods (*11*). Very high values were obtained for the concentration of GABA and activity of GAD in the islets of Langerhans (see Table 2); these values were one-tenth lower in the exocrine glands. The concentration of GABA in the islets corresponds to the concentration of GABA in the dorsal Deiters' nucleus and the dentate nucleus of the cerebellum, both of these areas having high concentrations of GABA with respect to the regional distribution of this compound in the mammalian brain (*3, 12*).

An insulinoma, β-cell tumor, of human pancreas (*13*), which was showing clinical manifestations, was surgically excised for therapeutic purposes. The tumor was removed together with a region of tissue surrounding it. The whole tissue block was immediately frozen in liquid nitrogen and GABA and GAD in the tissue were determined as described above. Histological examination revealed it to be an adenoma of the islets of Langerhans. The β-cells normally found only in Langerhans' islets had multiplied tremendously and had compressed the exocrine glands around the border of the tumor, and the tumor itself was heavily vascularized. Table 1 shows that the insulin content of the tumor region was considerably higher than that of the nontumor region, when measured on a wet weight basis (*14*). The tumor site and nontumor region of freeze-dried sections were easily differentiated under the stereomicroscope. The freeze-dried tissue was dissected into five parts (see Table 1, measurements 2 through 6) for assay. The GABA concentration and GAD activity in the nontumor region of the human pancreas were in good agreement with those of rat pancreas (Table 1, measurement 1). In contrast, both the GABA content and GAD activity in the tumor region were strikingly high compared with those of the nontumor region and were even higher than those of rat pancreatic islets. The border area between the tumor and the nontumor region (measurement 4) showed variable GABA content ranging from 6.2 to 18.8 mmole kg^{-1}. It is interesting that the area that included mainly tumor cells (measurement 6) contained 28 to 55 mmole of GABA per kilogram, which was much higher than that of the area with blood capillaries (measurement 5) whose GABA concentration and GAD activity were almost the same as those in the whole tumor region (measurement 3). Although the GABA content of the Langerhans' islets of human pancreas was not determined, the high concentration of GABA and the high GAD activity in the insulinoma suggest that Langerhans' islets in the human pancreas normally contain high concentrations of GABA, as rat pancreatic islets do.

Concerning the localization of GABA in the CNS, it is generally considered that GABA is located mainly in nerve endings of inhibitory neurons (*2, 3*). This possibility cannot be excluded in the case of pancreas. Sympathetic and cholinergic nerve fibers innervate the pancreatic islets and modify to some extent the release of insulin from the islets (*15*). The precise localization and role of GABA in pancreas has not been described, however. Recently we studied the effect of streptozotocin on the GABA concentration in the rat pancreatic islets (*16*). Streptozotocin is considered to attack β-cells in the islets (*17*). Seven hours after the intravenous administration of streptozotocin (65 mg kg^{-1}), the level of GABA in the islets decreased to 10 percent of the original level, whereas the GABA content in the exocrine glands did not show any remarkable change. Together with the finding of the high content of

Table 1. Concentration of GABA and activity of GAD in rat pancreas and in a human insulinoma. Values are means ± standard error. Numbers in parentheses show the number of samples assayed. (Measurement 1) The whole pancreas of the rat included the endocrine and exocrine glands. (Measurements 2 to 6) The freeze-dried section of the human pancreas was dissected into five parts: a nontumor region with histologically normal pancreatic structure; a tumor region (adenoma of β-cells with abundant capillary vascularization); a border area between the tumor and nontumor region; another small area of tumor region including tumor cells and blood vessels; and a small tumor region consisting mainly of tumor cells without blood vessels. GABA and GAD in measurements 1 to 3 (100- to 200-μg samples, dry weight) were determined by the direct GABA and GAD assay method without enzymatic NADPH cycling, and in measurements 4 to 6 (50- to 100-ng samples) by the microassay for GABA with enzymatic NADPH cycling. All these determinations were made with freeze-dried tissue. The content of insulin was determined in wet tissue of the same region by acid-ethanol extraction and radioimmunological assay.

Measurement	Region of pancreas	GABA (mmole kg^{-1})	GAD ($mmole_{GABA}$ kg^{-1} $hour^{-1}$)	Insulin [unit g^{-1} (wet weight)]
		Rat		
1	Whole pancreas	2.51 ± 0.33 (5)	2.58 (5)	
		Human being		
2	Nontumor region	2.81 ± 0.31 (5)	2.01 (7)	3.93 ± 0.12 (4)
3	Tumor region	25.47 ± 0.41 (7)	138.2 (8)	12.00 ± 0.39 (4)
4	Border area	12.96 ± 2.58 (5)		
5	Area of tumor site with capillaries	25.73 ± 0.61 (5)		
6	Area consisting mainly of tumor cells	38.44 ± 3.35 (6)		

Table 2. Concentration of GABA and activity of GAD in Langerhans' islets and exocrine glands (acini) of rat pancreas. Values are means ± standard error. Tissue was measured as dry weight. Numbers in parentheses show the number of samples isolated from each rat. GAD activity is expressed as amount of GABA produced per kilogram of tissue (dry weight) per hour. GABA and GAD were determined by the microassay of GABA with enzymatic cycling of NADPH.

Rat	Islets of Langerhans		Acini	
	GABA (mmole kg^{-1})	GAD ($mmole_{GABA}$ kg^{-1} $hour^{-1}$)	GABA (mmole kg^{-1})	GAD ($mmole_{GABA}$ kg^{-1} $hour^{-1}$)
A	16.3 ± 1.4 (27)	65.6 (10)	1.45 ± 0.40 (13)	3.71 (9)
B	17.8 ± 1.8 (19)	62.1 (16)	2.00 ± 0.61 (8)	5.67 (17)
C	23.0 ± 2.9 (18)	70.5 (27)	2.54 ± 0.28 (15)	3.49 (21)
D	19.5 ± 3.0 (12)	63.1 (18)	2.73 ± 0.34 (7)	4.72 (10)
E	19.9 ± 1.3 (16)	72.4 (5)	1.13 ± 0.18 (9)	5.78 (12)
Average	18.9 ± 0.9 (92)	66.7 (76)	1.97 ± 0.19 (52)	4.67 (77)

GABA and high activity of GAD in the β-cell tumor, this result suggests that GABA is synthesized and localized within β-cells in the islets and probably does not originate in the nerve terminals as in the CNS. In the islets, GABA may be involved in functions such as the synthesis and release of insulin, the synthesis of protein, the supply of energy through the GABA shunt, or neurotransmission as in the CNS. Recently, other pathways of GABA synthesis have been reported, from putrescine (*18*) and glutamate (*19*). Although we found high GAD activity in the islets of Langerhans in parallel with the presence of high amounts of GABA, part of the GABA found in the islets may be derived through these other pathways. Further studies of the function and distribution of GABA in the pancreatic islets might clarify the role of GABA in the mammalian CNS.

YASUHIRO OKADA
HIROSHI TANIGUCHI
CHICACO SHIMADA

Department of Neurochemistry, Tokyo Metropolitan Institute for Neurosciences, 2-6, Musashidai, Fuchu-shi, Tokyo, Japan, and *Department of Internal Medicine, Kobe University School of Medicine, Ikuta-Ku, Kobe, Japan*

References and Notes

1. E. Roberts, in *GABA in Nervous System Function*, E. Roberts, T. N. Chase, A. B. Tower, Eds. (Raven, New York, 1976), pp. 1–5.
2. M. Otsuka, in *Structure and Function of Nervous Tissue*, G. H. Bourne, Ed. (Academic Press, New York, 1972), vol. 4, pp. 249–289.
3. Y. Okada, in *GABA in Nervous System Function*, E. Roberts, T. N. Chase, A. B. Tower, Eds. (Raven, New York, 1976), pp. 235–243.
4. M. Zackmann, P. Tocci, W. L. Nyhan, *J. Biol. Chem.* **241**, 1355 (1966); B. Harber, K. Kuriyama, E. Roberts, *Biochem. Pharmacol.* **19**, 1119 (1970).
5. N. Seiler and M. Wiechmann, *Hoppe-Seyler's Z. Physiol. Chem.* **350**, 1493 (1969); D. F. Whelan, C. R. Scriber, F. Mohyuddin, *Nature (London)* **244**, 916 (1969).
6. H. H. Tallan, S. Moore, W. H. Stein, *J. Biol. Chem.* **211**, 927 (1954).
7. R. J. Drummond and A. T. Phillips, *J. Neurochem.* **23**, 1207 (1974).
8. Y. Okada, H. Taniguchi, Ch. Shimada, F. Kurosawa, *Proc. Jpn. Acad.* **51**, 760 (1975).
9. Y. Okada, *Brain Res.* **75**, 362 (1974); ——— and Ch. Shimada, *ibid.* **98**, 202 (1975).
10. O. H. Lowry and J. V. Passonneau, *A Flexible System of Enzymatic Analysis* (Academic Press, New York, 1972).
11. Y. Okada and N. Seiler, in preparation.
12. Y. Okada and Ch. Shimada, *Brain Res.* **107**, 678 (1976).
13. The surgical specimen was supplied Dr. K. Ohnishi, Kobe Rosai Hospital, Kobe, Japan.
14. We thank Y. Watanabe, A Tsutou, M. Hasegawa, M. Seki, K. Murakami, and T. Kobayashi for their assistance in insulin assay.
15. S. C. Woods and D. Porte, Jr., *Physiol. Rev.* **54**, 596 (1974).
16. Y. Okado and H. Taniguchi, in preparation.
17. R. N. Arison, E. I. Ciaccio, M. S. Glitzer, J. A. Cassaro, M. P. Pruss, *Diabetes* **16**, 51 (1976).
18. N. Seiler and M-J. Al-Therib, *Biochem. J.* **144**, 29 (1974).
19. N. Seiler and G. Wagner, *Neurochem. Res.* **1**, 113 (1976).
20. We thank Drs. G. Takagaki and P. Haug for discussions and criticism. Supported in part by a grant from the Japanese Ministry of Education.

11 May 1976; revised 8 July 1976

Amianthoid Change: Orientation of Normal Collagen Fibrils During Aging

Abstract. *High-angle x-ray diffraction provides direct evidence that amianthoid change, occurring during aging of costal cartilage, corresponds to a transformation from an isotropic to a marked anisotropic distribution of collagen fibrils. Low-angle x-ray diffraction and electron microscopy show that the fibrils have the customary 67-nanometer axial periodicity. Electron microscopy shows that wide amianthoid collagen fibrils consist of smaller parallel fibrils fused together. Similarities between amianthoid change and tendon morphogenesis are briefly discussed. Amianthoid change is remarkable in that aging is accompanied by increased order.*

We have used x-ray diffraction and electron microscopy to investigate the amianthoid changes that occur during the aging of costal (rib) cartilage. Amianthoid areas are seen as opaque white flecks in the surrounding yellow, translucent hyaline cartilage (*1*); under the light microscope they have a fibrous appearance, which has led to the terms "fibrillation," "fibrillary transformation," and "fibrous transformation" for the changes (*2*). It has been postulated that age-dependent changes may be the first stage in the development of osteoarthrosis (osteoarthritis) which occurs when the articular cartilage lining synovial joints is eroded (*3*).

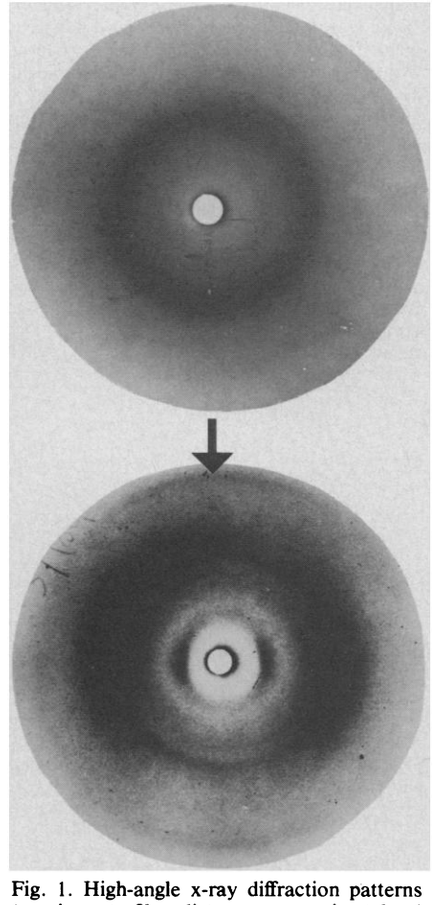

Fig. 1. High-angle x-ray diffraction patterns (specimen-to-film distance approximately 4 cm) from cartilage in transverse section of rib. (Top) There is no sign of orientation in the organization of the fibrils in the cartilage. (Bottom) The pattern from an amianthoid area is diagnostic of oriented collagen; the arrow points to the characteristic 0.29-nm meridional reflection.

Our high-angle x-ray diffraction patterns, obtained from the cartilage in transverse sections of human rib (*4*), provide new and direct evidence that amianthoid areas consist of oriented collagen fibrils. Although patterns from normal areas (Fig. 1, top) show no detectable orientation in any of their components, the patterns (Fig. 1, bottom) from amianthoid areas are clearly characteristic—in general, in intensity distribution, and, in particular, in the 0.29-nm meridional reflection—of partially oriented collagen fibrils (*5*). According to criteria listed by Ramachandran (*6*) this result provides direct evidence (so far as we know, the first) for amianthoid areas consisting of oriented collagen fibrils; additional direct evidence comes from our low-angle x-ray diffraction patterns and electron micrographs. Previously, the only available evidence for amianthoid areas consisting of collagen was from enzymatic studies and electron microscopy (*2*).

Low-angle x-ray diffraction patterns of amianthoid areas show that their oriented collagen fibrils have an axial periodicity which is not significantly different from that expected of normal fibrils. Measurements of electron micrographs of thin sections of fixed and stained amianthoid areas had previously suggested that their fibril periodicities were shorter than usual at between 56 and 62 nm (*2*). It is notoriously difficult to obtain accurate estimates of periodicity from micrographs of sectioned material in which, for example, fibrils may not have been cut exactly longitudinally. Further, the material has to be subjected to considerable chemical treatment, including exhaustive dehydration. X-ray diffraction measurements do not suffer from such drawbacks. Figure 2 shows that our patterns yield a value of 67 ± 1 nm for the periodicity of amianthoid collagen fibrils (*7*). This value is clearly comparable to values obtained for tendon collagen (*8*, *9*). Unfortunately, no com-